https://doi.org/10.5194/egusphere-2026-6485
Preprint. Discussion started: 9 November 2026
© Author(s) 2026. CC BY 4.0 License.

Chemical and dynamical controls on rapid secondary organic aerosol accumulation over a large lake in eastern China

Zeyuan Tian[1,2,3], Jiaping Wang*[,1,2,3], Dian Ding[2,3], Ke Ding[1,2], Jiandong Wang[4,5], Lei Yao[6,7], Chuang Li[8], Gan Yang[8], Jiayi Zhou[8], Ning Wang[8], Yuliang Liu[2,3], Tengyu Liu[2,3], Wei Nie[2,3], Chao Yan[3,9], Jinbo Wang[2,3,a], Qihao Lin[1,2], Zhouyang Zhang[4,5], Bin Wang[4,5], Chang Zhou[2,3], Caijun Zhu[2,3], Zhenning Wang[2,3], Jianxun Wang[3,9], Lin Wang[7,8,10,11], Xin Huang[1,2]

[1]State Key Laboratory of Severe Weather Meteorological Science and Technology, Nanjing University, Nanjing 210023, China
[2]Joint International Research Laboratory of Atmospheric and Earth System Sciences, School of Atmospheric Sciences, Nanjing University, Nanjing 210023, China
[3]National Observation and Research Station for Atmospheric Processes and Environmental Change in Yangtze River Delta, Nanjing 210023, China
[4]State Key Laboratory of Climate System Prediction and Risk Management, Nanjing University of Information Science and Technology, Nanjing 210044, China
[5]Collaborative Innovation Center on Forecast and Evaluation of Meteorological Disasters, School of Atmospheric Physics, Nanjing University of Information Science and Technology, Nanjing 210044, China
[6]Shanghai Key Laboratory of Air Quality and Environmental Health, Department of Environmental Science and Engineering, Jiangwan Campus, Fudan University, Shanghai 200438, China
[7]Shanghai Institute of Pollution Control and Ecological Security, Shanghai 200092, China
[8]Department of Environmental Science and Engineering, Fudan University, Shanghai 200433, China
[9]Nanjing-Helsinki Institute in Atmospheric and Earth System Sciences, Nanjing University, Nanjing 210023, China
[10]National Observations and Research Station for Wetland Ecosystems of the Yangtze Estuary, Shanghai 200438, China
[11]IRDR International Center of Excellence on Risk Interconnectivity and Governance on Weather/Climate Extremes Impact and Public Health, Fudan University, Shanghai 200438, China
[a]now at: National Satellite Meteorological Center (National Center for Space Weather), China Meteorological Administration, Beijing 100081, China

Correspondence to: Jiaping Wang (wangjp@nju.edu.cn)

Abstract. Lake-induced meteorological conditions can influence the formation and spatial distribution of secondary organic aerosol (SOA) by modulating precursor mixing, chemical processing, and aerosol transport. Yet how these processes act together to drive rapid SOA accumulation remains insufficiently understood. Here we conducted comprehensive measurements of aerosol composition at Taihu Lake in the Yangtze River Delta during the summer of 2023. Throughout the campaign, organic aerosol (OA) dominated submicron particulate matter (PM_1) mass, accounting for 56% of the total PM_1 (compared to 41% at a nearby suburban station), with secondary components comprising 84% of the total OA at Taihu Lake. During a prominent pollution episode (August 10–12), OA reached 73.7 μg m^{-3} (78% of PM_1), and the SOA fraction rose to 90%. This rapid SOA accumulation was driven by a unique physicochemical synergy at the lake-land interface. The convergence of anthropogenic and biogenic emissions supplied a highly reactive precursor pool, while enhanced atmospheric oxidation capacity promoted rapid oxidation and aerosol aging, leading to efficient SOA formation. As revealed by modeling analyses, the lake–land thermal contrast further drove a pronounced lake–land breeze circulation, inducing localized subsidence over

https://doi.org/10.5194/egusphere-2026-6485
Preprint. Discussion started: 9 November 2026
© Author(s) 2026. CC BY 4.0 License.

the lake that efficiently transported SOA formed aloft down to the surface, thereby favoring its rapid accumulation. These findings suggest that lake environments can provide favorable chemical and meteorological conditions for efficient SOA production, highlighting the need to consider large inland lakes in assessments of regional aerosol chemistry and air quality.

1 Introduction

Organic aerosol (OA) constitutes a substantial fraction of atmospheric fine particulate matter ($PM_{2.5}$), exerting profound impacts on air quality, regional climate forcing, and human health (Huang et al., 2014; Jacobson et al., 2000; Jimenez et al., 2009). Secondary organic aerosol (SOA), formed through the atmospheric oxidation of volatile organic compounds (VOCs), represents a major component of OA (Carlton et al., 2009; Hallquist et al., 2009; Ying et al., 2015). Although stringent emission reduction measures in China have led to a decline in total $PM_{2.5}$ mass, the relative contribution of SOA has exhibited a persistent upward trend. SOA has consequently emerged as the primary driver of haze episodes (Chen et al., 2024; Huang et al., 2014). SOA formation is a complex process governed by the synergistic interplay between precursor emissions, atmospheric oxidation capacity (AOC), and meteorological conditions (Gu et al., 2023; Hu et al., 2017; Huang et al., 2025; Lee et al., 2016; RenHe et al., 2014; Sun et al., 2025). Elucidating SOA formation pathways across diverse regional environments is therefore critical for effective pollution mitigation strategies.

The Yangtze River Delta (YRD), one of China's most industrialized and densely populated regions, faces persistent challenges from the compound pollution of ozone (O_3) and fine particulate matter ($PM_{2.5}$) (Lu et al., 2018; Ming et al., 2017; Xie et al., 2021; Zhang et al., 2022; Zhou et al., 2025). Taihu Lake, a major freshwater body located in the heart of the YRD, represents a typical lake-urban environment. In this distinct environment, anthropogenic plumes from surrounding megacities intersect with biogenic emissions from both aquatic and terrestrial vegetation, creating a complex precursor pool for SOA formation (Yu et al., 2019). Previous studies have reported elevated O_3 concentrations in the Taihu Lake region (Shao et al., 2025; Zhang et al., 2017), where elevated O_3 levels not only pose direct health risks but also contribute to higher AOC (Liu et al., 2022), thereby promoting the oxidation of VOCs into SOA (Feng et al., 2019). Furthermore, the lake environment introduces specific meteorological and chemical conditions that may influence aerosol formation and evolution (Cleary et al., 2022). The thermal properties of the lake surface can affect boundary layer development and pollutant accumulation, while mesoscale circulations, such as lake-land breezes, may further facilitate the recirculation of air masses and pollutants within the lake boundary layer (Brook et al., 2013; Hayden et al., 2011; Levy et al., 2010). High humidity over the water surface potentially promotes heterogeneous or aqueous-phase reaction pathways (Ervens et al., 2011; Huang et al., 2020; Kuang et al., 2020). However, quantitative evidence on how elevated AOC and lake-induced boundary layer dynamics affect SOA formation in the Taihu Lake region remains limited.

https://doi.org/10.5194/egusphere-2026-6485
Preprint. Discussion started: 9 November 2026
© Author(s) 2026. CC BY 4.0 License.

In this study, we conducted a comprehensive field campaign during the summer of 2023 at Taihu Lake to systematically characterize the chemical evolution of SOA and associated precursor chemistry. By integrating field observations with the regional meteorological and chemical transport model simulations, we investigated a typical SOA formation episode to elucidate the interplay between the photochemical oxidation of mixed anthropogenic-biogenic precursors and lake-induced meteorological processes. Our findings advance the mechanistic understanding of SOA formation in lake-influenced environments, with important implications for air quality management at complex lake–land interface regions.

2 Materials and methods

2.1 Sampling site and field measurements

Field observations were conducted from July 13 to August 31, 2023, at the Taihu Laboratory for Lake Ecosystem Research, Chinese Academy of Sciences. The station is located on the eastern shore of Meiliang Bay, Taihu Lake (120.22°E, 31.42°N, Fig. S1), in the southwestern suburbs of Wuxi, Jiangsu Province (hereafter referred to as the Taihu station). Situated in a sparsely populated area around the lake, with no major industrial sources nearby, this station provides an ideal platform to investigate the complex interaction between lake-induced meteorological conditions and the chemical evolution of urban-derived pollutant plumes.

A comprehensive suite of instruments was deployed to characterize aerosol properties and atmospheric composition. A Soot Particle Aerosol Mass Spectrometer (SP-AMS, Aerodyne Research Inc., USA) was operated at a temporal resolution of 1 minute in mass-sensitive V mode, alternating between laser-on and laser-off modes at 5-minute intervals, to simultaneously measure black carbon (BC) and non-refractory species including organics, sulfate, nitrate, ammonium, and chloride. To characterize gaseous oxygenated organic molecules (OOMs) associated with SOA formation, a nitrate-chemical ionization-atmospheric pressure interface-long-time-of-flight (nitrate-CI-APi-LToF) was used. O_3 concentrations were monitored using an ultraviolet photometric analyzer (Thermo Environmental Instruments, TEI Inc., model 49i). The particle number size distributions were measured over a broad size range. An Airmodus A10 particle size magnifier (PSM) was employed to measure sub-3 nm particles, while two scanning mobility particle sizers (nano-SMPS and long-SMPS, TSI Inc., USA) measured the size distributions in the 3–736 nm range.

For comparison, synchronous datasets from the Station for Observing Regional Processes of the Earth System (SORPES) were utilized to provide a reference for a typical suburban background environment. SORPES station is located at Nanjing University Xianlin Campus (118.95°E, 32.12°N), approximately 150 km northwest of the Taihu station. Detailed descriptions of the SORPES station have been provided in previous studies (Ding et al., 2016, 2019). At SORPES station, non-refractory $PM_{2.5}$ species and BC were measured using a time-of-flight aerosol chemical speciation monitor (TOF-ACSM) and a multi-wavelength aethalometer (model AE33, Magee Scientific Corporation, California, USA), respectively. Similar to the Taihu

https://doi.org/10.5194/egusphere-2026-6485
Preprint. Discussion started: 9 November 2026
© Author(s) 2026. CC BY 4.0 License.

station, ambient OOMs at SORPES station were characterized using a chemical ionization atmospheric pressure interface time-of-flight mass spectrometer with nitrate reagent ions (nitrate-CI-APi-ToF; Aerodyne Research Inc. and Tofwerk AG) (Liu et al., 2021, 2023).

2.2 Data analysis and model simulations

The SP-AMS data were processed using standard time-of-flight AMS data analysis software packages (SQUIRREL v1.60P and PIKA v1.20P) to quantify the mass concentrations of submicron particulate matter (PM_1) chemical components. The relative ionization efficiencies (RIE) for ammonium and sulfate were determined to be 4.32 and 1.32 using pure NH_4NO_3 and $(NH_4)_2SO_4$ particles, respectively. Default RIEs of 1.4 for organics, 1.1 for nitrate, and 1.3 for chloride were applied. The mass ionization efficiency for refractory black carbon, mIE_{rBC}, was calibrated by sampling monodisperse 300 nm Regal Black particles (Onasch et al., 2012). A collection efficiency (CE) of 0.5 was applied in this study. For source apportionment, positive matrix factorization (PMF) was performed on the high-resolution organic mass spectra obtained in laser-off mode, using the PMF Evaluation Tool (PET, v3.04A) (Paatero and Tapper, 1994; Ulbrich et al., 2009). Four distinct OA factors were identified (see Sect. S2 in the Supplement), including hydrocarbon-like OA (HOA), less-oxidized oxygenated OA (LO-OOA), and two more-oxidized oxygenated OA factors (MO-OOA1 and MO-OOA2).

To quantify the gas-to-particle partitioning potential of OOMs detected by the nitrate-CI-APi-LToF, we used two volatility basis set (VBS) parameterizations to estimate the volatility of monoterpene-derived OOMs and other OOM types following established methods (Donahue et al., 2011; Mohr et al., 2019; Nie et al., 2022; Tröstl et al., 2016). Following the approach described by Nie et al. (2022), detected OOMs were classified according to their likely VOC precursor classes based on their molecular composition, including aliphatics, aromatics, isoprene, and monoterpenes.

To evaluate the impact of regional transport on aerosols at Taihu Lake, the Community Multiscale Air Quality (CMAQ v5.5) model, driven by the Weather Research and Forecasting (WRF v4.5) model, was employed to simulate the spatiotemporal distribution of pollutants over the Yangtze River Delta. Both models were configured with three nested domains (27 km, 9 km, and 3 km; Fig. S5), with meteorological initial and boundary conditions derived from ERA5 reanalysis data, and four-dimensional data assimilation (FDDA) was applied to constrain the WRF simulations. For the chemical transport simulation, anthropogenic emissions were obtained from the ABaCAS-EI v2.0 inventory (domestic) and the Emissions Database for Global Atmospheric Research (EDGAR) (international), while biogenic emissions were calculated using the Model of Emissions of Gases and Aerosols from Nature (MEGAN v2.10). Furthermore, the meteorological fields simulated by WRF were analyzed to characterize the lake-induced meteorological conditions during the study period. Backward trajectory analysis was performed using the Hybrid Single-Particle Lagrangian Integrated Trajectory model (HYSPLIT, NOAA-ARL) driven by meteorological input data from the Global Data Assimilation System (GDAS1, 1° resolution) (Stein et al., 2015). To trace the transport pathways of air masses arriving at Taihu Lake, 24-hour backward trajectories were calculated every 3

https://doi.org/10.5194/egusphere-2026-6485
Preprint. Discussion started: 9 November 2026
© Author(s) 2026. CC BY 4.0 License.

hours with a starting height of 100 m above ground level. Detailed model configurations are provided in Sect. S3 in the Supplement.

3 Results and discussion

3.1 Mass concentrations and chemical composition

The temporal variations of PM_1 chemical components throughout the campaign are shown in Fig. 1. Total PM_1 mass concentrations ranged from 1.9 to 94.9 μg m^{-3} during the campaign. OA was the predominant constituent, with concentrations varying from 0.4 to 73.7 μg m^{-3}, and generally accounted for the largest fraction of PM_1, particularly during pollution episodes. Notably, during the pollution episode from August 10 to 12, OA exhibited a synchronous but more pronounced increase compared to inorganic species, thereby emerging as the principal contributor to PM_1 accumulation. In contrast, during clean periods (e.g., July 26–31), the average PM_1 concentration decreased to 5.8±3.9 μg m^{-3}. Under these conditions, the relative contribution of OA decreased, whereas secondary inorganic aerosols (SIA), particularly sulfate, substantially increased. The diurnal variations of aerosol species are presented in Fig. S9. OA displayed a pronounced diurnal pattern, peaking at approximately 11:00 local time (LT), with a more prominent daytime enhancement during pollution episodes.

Measurements at Taihu station were compared with those at the SORPES station. During the campaign, Taihu station recorded an average PM_1 concentration of 16.8±12.1 μg m^{-3}, which was comparable to the $PM_{2.5}$ concentration at SORPES station (19.4±10.1 μg m^{-3}) (Fig. 1c). However, the two sites exhibited different aerosol chemical compositions. OA accounted for an average of 56% of the total mass at Taihu station, considerably higher than the 41% observed at SORPES station (Fig. 1d). This contrast indicates that organic components contribute substantially more to aerosol mass in the lake environment than in suburban areas, highlighting the potentially intensified formation of SOA at this distinct urban-lake interface.

https://doi.org/10.5194/egusphere-2026-6485
Preprint. Discussion started: 9 November 2026
© Author(s) 2026. CC BY 4.0 License.

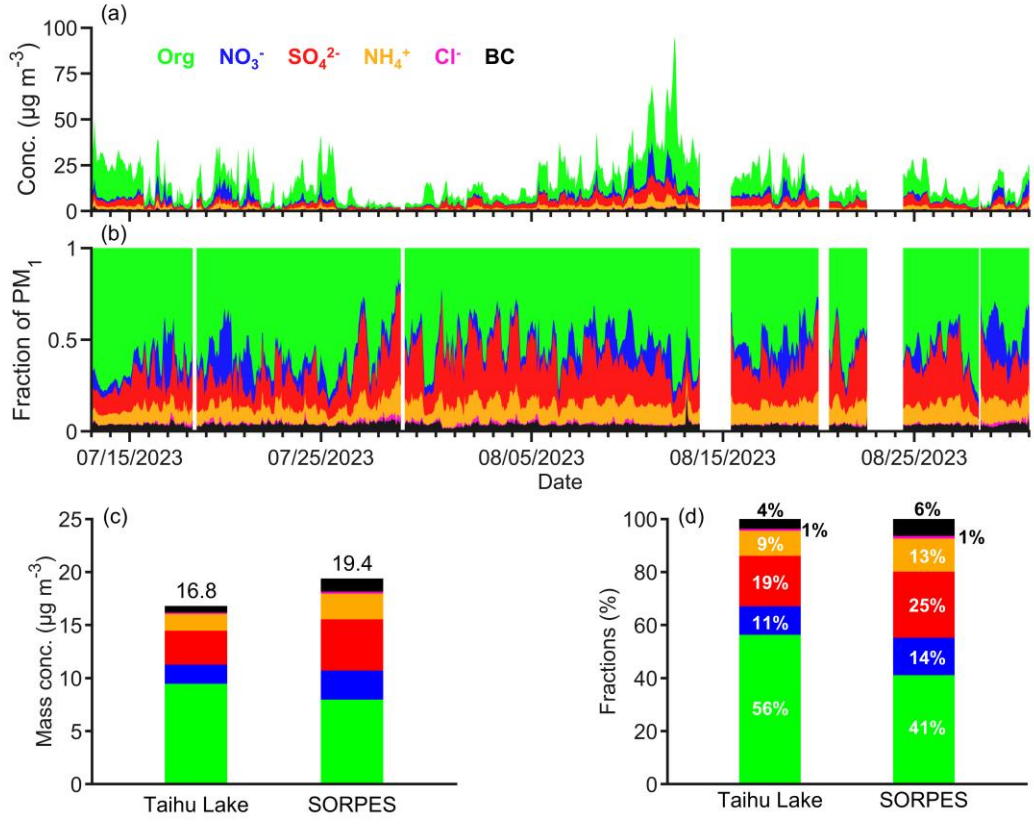


Figure 1. Time series of (a) mass concentrations and (b) mass fractions of PM_1 chemical species at Taihu station during the campaign. Average (c) mass concentrations and (d) mass fractions of chemical components in PM_1 at Taihu station and $PM_{2.5}$ at SORPES station.

The spatial heterogeneity of atmospheric oxidation capacity and $PM_{2.5}$ across the YRD was further explored by comparing observations at Taihu station with those from six representative national monitoring stations (Wuxi, Suzhou, Hangzhou, Taizhou, Shanghai, and Xuancheng; Fig. 2d). Odd oxygen ($O_x = O_3 + NO_2$) is a commonly used proxy for photochemical activity and atmospheric oxidative environment, as it accounts for the titration of O_3 by NO (Herndon et al., 2008). Among all seven stations, Taihu station recorded the highest daily O_x concentration on 89% of the valid observation days, with O_x exceeding 40 μg m^{-3} on 27% of days (Fig. 2a). Consistent with this, the daily difference in O_x concentration (ΔO_x) between Taihu station and the median of the six surrounding stations remained positive throughout the campaign (Fig. 2b). This consistently higher O_x concentration suggests enhanced photochemical activity at Taihu Lake, providing favorable conditions for the formation of SOA. Correspondingly, $\Delta PM_{2.5}$ (Fig. 2c), defined as the difference between $PM_{2.5}$ concentrations at Taihu station and the median of the six surrounding stations, was positive on 70% of the valid observation days, indicating generally higher particle loadings over the lake, with particularly pronounced elevations during August 10–12.

https://doi.org/10.5194/egusphere-2026-6485
Preprint. Discussion started: 9 November 2026
© Author(s) 2026. CC BY 4.0 License.

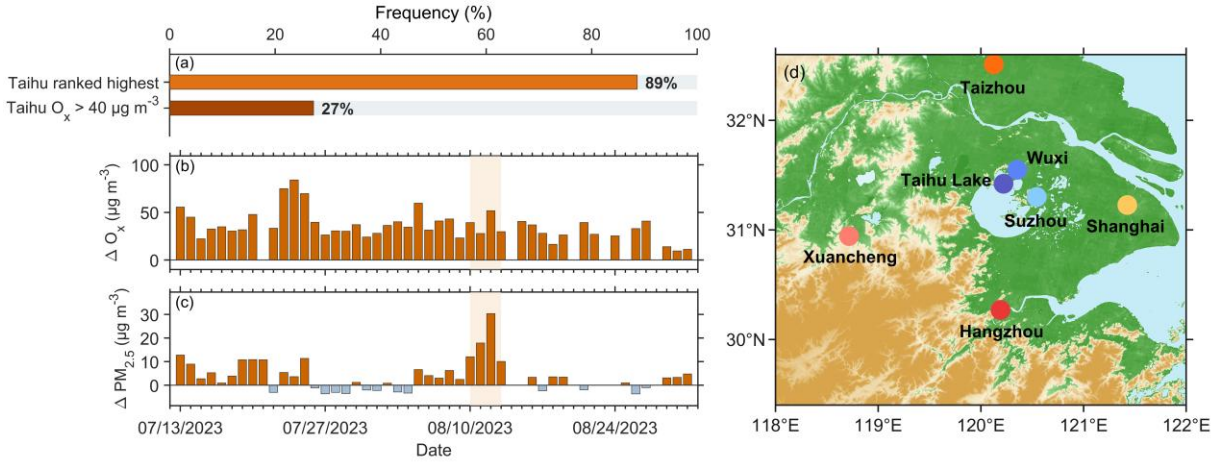


Figure 2. (a) Frequency statistics characterizing the relative photochemical intensity of O_x at Taihu station compared with the six surrounding stations, including the fraction of valid days on which Taihu station recorded the highest daily O_x concentration among all seven stations, and the fraction of valid days on which O_x at Taihu station exceeded 40 μg m^{-3} (b) Daily difference in odd oxygen (O_x = O_3 + NO_2) concentration (ΔO_x) between Taihu station and the median O_x concentration of six representative national monitoring stations. (c) Daily difference in $PM_{2.5}$ concentration ($\Delta PM_{2.5}$) between Taihu station and the median $PM_{2.5}$ concentration of the same six stations ($PM_{2.5}$ concentrations at Taihu station were converted from PM_1 measurements, see Sect. S5 in the Supplement for details). Daily values in (a)–(c) are calculated for days with at least 18 common valid hours, defined as hours with valid O_x measurements at Taihu station and at least four of the six surrounding stations. In (b) and (c), the shaded regions denote the pollution episode of August 10–12. (d) Geographic locations of Taihu station and six surrounding national monitoring stations across the Yangtze River Delta.

3.2 Investigating OA sources with PMF

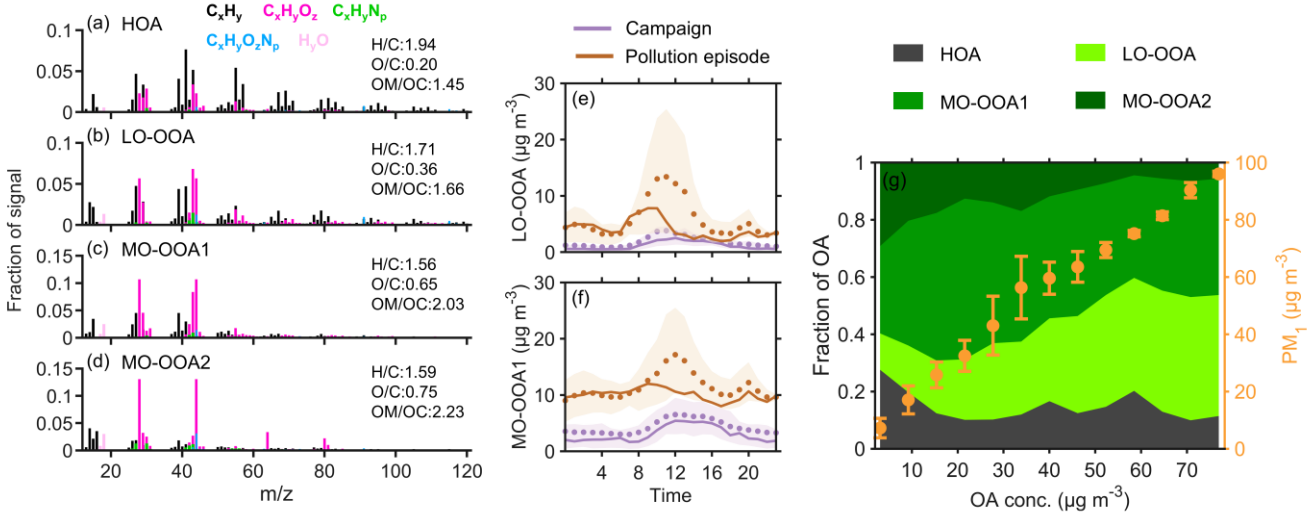
The mass spectra of individual PMF factors are shown in Figs. 3a–d, with their temporal variations presented in Fig. S11. HOA, representing primary emissions (H/C = 1.94, O/C = 0.20), showed strong correlations with combustion tracers (r_{BC} = 0.5, r_{NO_x} = 0.54; Table S3). On average, HOA accounted for 16.4% of the total OA mass throughout the campaign, with the highest contribution (~28%) occurring in the morning, consistent with traffic emissions, while it reached a minimum (~7%) in the afternoon following boundary layer development (Figs. S12 and S13). The three oxygenated OA (OOA) factors, which accounted for an average of 83.6% of total OA, represented different stages of atmospheric aging. Among them, MO-OOA2 exhibited the highest oxidation state (O/C = 0.75) and a strong correlation with sulfate ($r_{SO_4^{2-}}$= 0.94), characterizing it as a highly aged SOA, likely associated with long-range transport. LO-OOA (O/C = 0.36) and MO-OOA1 (O/C = 0.65) were identified as fresh-to-intermediate photochemical SOA, as evidenced by their strong correlations with O_3 (r_{O_3} = 0.53 and 0.66, respectively).

The diurnal profiles of the two photochemically driven SOA factors (LO-OOA and MO-OOA1) exhibit distinct temporal patterns (Figs. 3e and 3f). Both factors increased rapidly after sunrise, coinciding with increasing solar radiation and O_3 levels. LO-OOA peaked at approximately 11:00 LT and subsequently declined, while MO-OOA1 remained at a high level until late afternoon (~16:00 LT). The high correlation between these two factors (r = 0.75), combined with the difference in their peak

https://doi.org/10.5194/egusphere-2026-6485
Preprint. Discussion started: 9 November 2026
© Author(s) 2026. CC BY 4.0 License.

195 times, suggests a potentially successive aging pathway. Under the highly oxidative environment at Taihu Lake, LO-OOA may undergo progressive conversion into MO-OOA1. The afternoon decrease in LO-OOA likely reflects this continuous photochemical aging, coupled with dilution as the planetary boundary layer develops.

The fractional distribution of OA components as a function of total OA loading is illustrated in Fig. 3g. Secondary components
200 consistently dominated the total OA mass, with their relative contribution further increasing at higher OA loadings. Specifically, the mass fraction of LO-OOA exhibited dramatic growth, rising from ~15% to over 40% as OA loading exceeded 50 μg m^{-3}. This pronounced increase underscores that the explosive SOA events at Taihu Lake may be primarily driven by rapid local accumulation of less-oxidized components, rather than merely the contribution of long-range transported air masses.



205 **Figure 3.** High-resolution mass spectra of the four identified OA factors: (a) hydrocarbon-like OA (HOA), (b) less oxidized oxygenated OA (LO-OOA), (c) more-oxidized oxygenated OA type 1 (MO-OOA1), and (d) more-oxidized oxygenated OA type 2 (MO-OOA2). (e–f) Diurnal variations of LO-OOA and MO-OOA1 during the whole campaign (purple) and pollution episodes (brown); the solid lines show median values, the shaded areas represent the interquartile range (25^{th}–75^{th} percentiles), and the markers represent mean values. (g) Mass fractions of the four OA components as a function of total OA loading. The average PM_1 concentrations within each bin are illustrated, with
210 error bars indicating the standard deviation of PM_1 concentrations.

3.3 Case study of rapid SOA formation

A prominent OA accumulation episode occurred from August 10 to 12, during which PM_1 concentrations rose rapidly to a peak of 94.9 μg m^{-3}, with a maximum hourly growth rate of 12.3 μg m^{-3} h^{-1}. During this episode, OA concentrations reached a maximum of 73.7 μg m^{-3}, accounting for 78% of PM_1 mass (Fig. 4c). Compared with the campaign average OA fraction of
215 56%, the OA fraction reached 66% on the pollution peak day (August 12), establishing OA as the primary contributor to aerosol loading (Fig. 4a). The SOA fraction (LO-OOA + MO-OOA1 + MO-OOA2) within OA increased to 90%, primarily driven by a rapid increase in the LO-OOA contribution (from 19% to 31%; Fig. 4b). Meanwhile, MO-OOA1 maintained a relatively constant mass fraction of 46%. Although its relative proportion remained unchanged, the absolute mass

https://doi.org/10.5194/egusphere-2026-6485
Preprint. Discussion started: 9 November 2026
© Author(s) 2026. CC BY 4.0 License.

concentration of MO-OOA1 increased rapidly on August 12 (Fig. 4d). The diurnal variations during this episode were more pronounced than the campaign-average patterns (Figs. 3e and 3f). OA concentrations exhibited a rapid daytime surge, primarily driven by the simultaneous increase in LO-OOA and MO-OOA1, indicating that enhanced photochemical activity played an important role in this pollution episode.

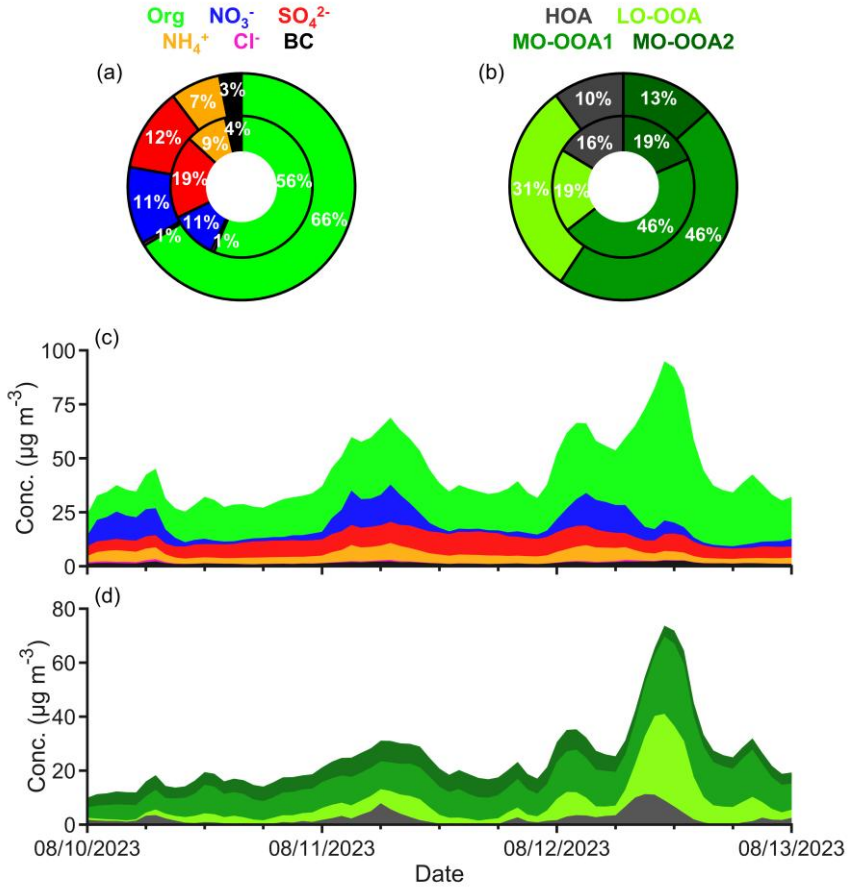


Figure 4. (a) Average chemical composition of PM_1 during the entire campaign (inner pie) and on the peak pollution day, August 12 (outer pie). (b) Average OA component fractions during the entire campaign (inner pie) and on August 12 (outer pie). Time series of (c) mass concentrations of PM_1 species and (d) OA components during the pollution episode (August 10–12).

To understand the chemical drivers behind the daytime SOA increase, we analyzed OOMs, which serve as critical intermediates in the transformation of VOCs to SOA (Ehn et al., 2014; Liu et al., 2023; Wang et al., 2022). During the August 10–12 episode, although the overall volatility distribution pattern remained consistent with the campaign average, the absolute mass concentrations of OOMs were substantially higher (Fig. 5). Concentrations of extremely low-volatility organic compounds (ELVOCs), low-volatility organic compounds (LVOCs), and semi-volatile organic compounds (SVOCs) increased by 10%, 20%, and 37%, respectively, compared to campaign-average levels. This overall elevation in OOM concentrations, particularly the larger relative enhancement in SVOCs, suggests more active photochemical processing during the pollution

https://doi.org/10.5194/egusphere-2026-6485
Preprint. Discussion started: 9 November 2026
© Author(s) 2026. CC BY 4.0 License.

episode, with substantial quantities of newly formed oxidation products potentially contributing to SOA formation. Compared with the suburban SORPES station, ultra-low volatility organic compound (ULVOC) concentrations at Taihu station were significantly higher. Similarly, ELVOC and LVOC concentrations at Taihu station exceeded those at SORPES station by an average of 66% and 63%, respectively, and remained 54% and 43% higher during the episode. Furthermore, SVOC concentrations at Taihu station exceeded those at SORPES station by 12% on average and by 17% during the pollution episode. Given the role of SVOCs as crucial intermediates in gas-to-particle partitioning, this enhancement indicates an elevated SOA formation potential at Taihu Lake under polluted conditions (Fig. S14). To further characterize OOMs across different volatility bins, we quantified the relative contributions of different precursor types within each bin. Although anthropogenic precursors predominated at both sites, the relative contributions of different precursor types varied between the two sites. Although anthropogenic precursors predominated at both sites, the relative contributions of different precursor types varied between the two sites. At Taihu station, the monoterpene-derived OOM fraction within ELVOCs was nearly twice that at the suburban SORPES station, suggesting a greater contribution from biogenic precursors. In addition, aromatic-derived OOMs accounted for a substantially larger fraction of ULVOCs at Taihu station, potentially reflecting the oxidation of anthropogenic aromatic precursors during transport from surrounding urban areas to Taihu Lake. This is consistent with the northerly winds prevailing during the early stage of the pollution episode (August 10; Fig. S15), which favored the transport of precursors from upwind urban areas toward Taihu Lake. These results highlight the contributions of both biogenic and anthropogenic precursors to SOA formation at the lake–urban interface.

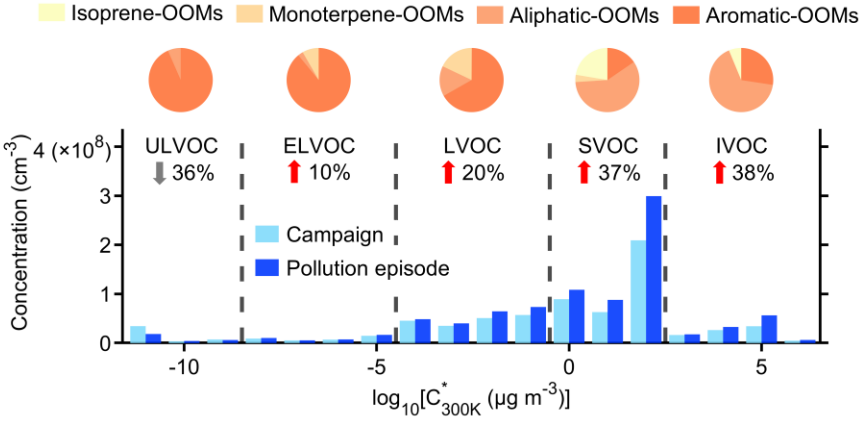


Figure 5. Volatility distribution of observed OOMs at 300 K during the entire campaign and the pollution episode, August 10–12. Pie plots show fractional contributions of different VOC precursor types (isoprene-OOMs, monoterpene-OOMs, aliphatic-OOMs, and aromatic-OOMs) to each volatility bin. The leftmost bin represents the sum of all components with $\log_{10}C^* < -10.5$.

The rapid accumulation of SOA was further facilitated by a distinctive meteorological regime over the lake. During the pollution episode, Taihu Lake was characterized by persistent high temperatures, elevated relative humidity, and stagnant surface wind (averaging ~2 m s^{-1}; Fig. S16). Owing to the high specific heat capacity of the lake water, the lake surface remained significantly cooler than the adjacent land during daytime, generating a pronounced lake–land thermal contrast (Fig.

https://doi.org/10.5194/egusphere-2026-6485
Preprint. Discussion started: 9 November 2026
© Author(s) 2026. CC BY 4.0 License.

6c). This cooler lake surface substantially reduced the sensible heat flux transferred to the overlying atmosphere, contributing to a markedly shallower planetary boundary layer over the lake compared with the surrounding land. As the lake-land thermal contrast intensified during daytime, surface winds diverged outward from the lake center (Fig. 6a), consistent with the markedly enhanced surface divergence observed over the lake around midday throughout the episode (Fig. 6b). The associated subsidence over the lake can further enhance SOA accumulation near the surface.

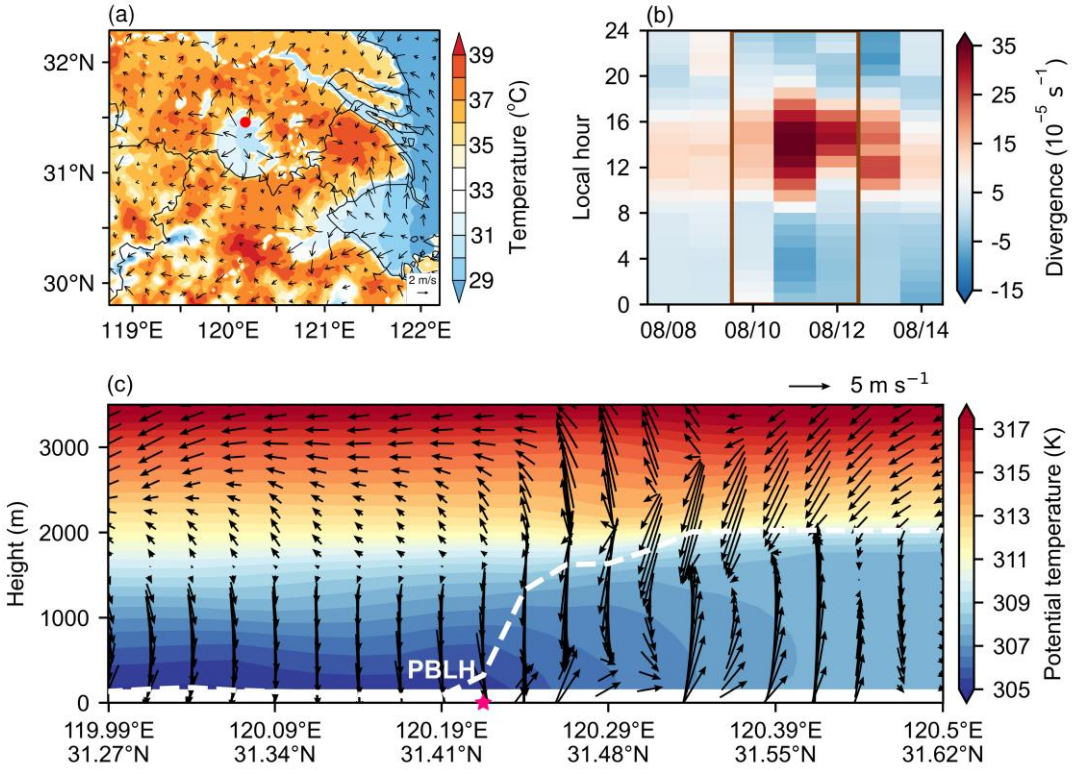


Figure 6. (a) Spatial distribution of WRF-simulated 2-m temperature (color shading) and 10-m wind field (vectors) at 14:00 LT on August 11. (b) Time series of WRF-simulated 10-m wind divergence over Taihu Lake as a function of local hour and date during August 8–14. The shaded region denotes the pollution episode of August 10–12. (c) Vertical cross-section through Taihu Lake showing WRF-simulated temperature (color shading) and wind field (vectors; vertical velocity magnified by a factor of 100 for visualization) at 14:00 LT on August 11. The dashed white line denotes the planetary boundary layer height (PBLH); the cross-section location is shown in Fig. S17.

This lake–land breeze-driven subsidence was further supported by model diagnostics. The simulated SOA vertical profiles and vertical wind fields showed predominantly downward motion below 2 km during the pollution episode (Fig. 7a), suggesting that downward transport may have contributed to near-surface SOA accumulation. Process analysis further indicated that vertical advection (ZADV) constituted the dominant positive contribution to the surface SOA budget during the episode, with a magnitude comparable to or exceeding the removal associated with horizontal advection (HADV) (Fig. 7b). This enhanced near-surface SOA accumulation may also have promoted further particle growth, consistent with the increase in the particle diameter from 119 to 171 nm between 06:00 and 12:00 LT on August 12 (Fig. S18). Overall, these findings highlight the role of lake–land breeze-induced subsidence in the rapid accumulation of SOA near the surface.

https://doi.org/10.5194/egusphere-2026-6485
Preprint. Discussion started: 9 November 2026
© Author(s) 2026. CC BY 4.0 License.

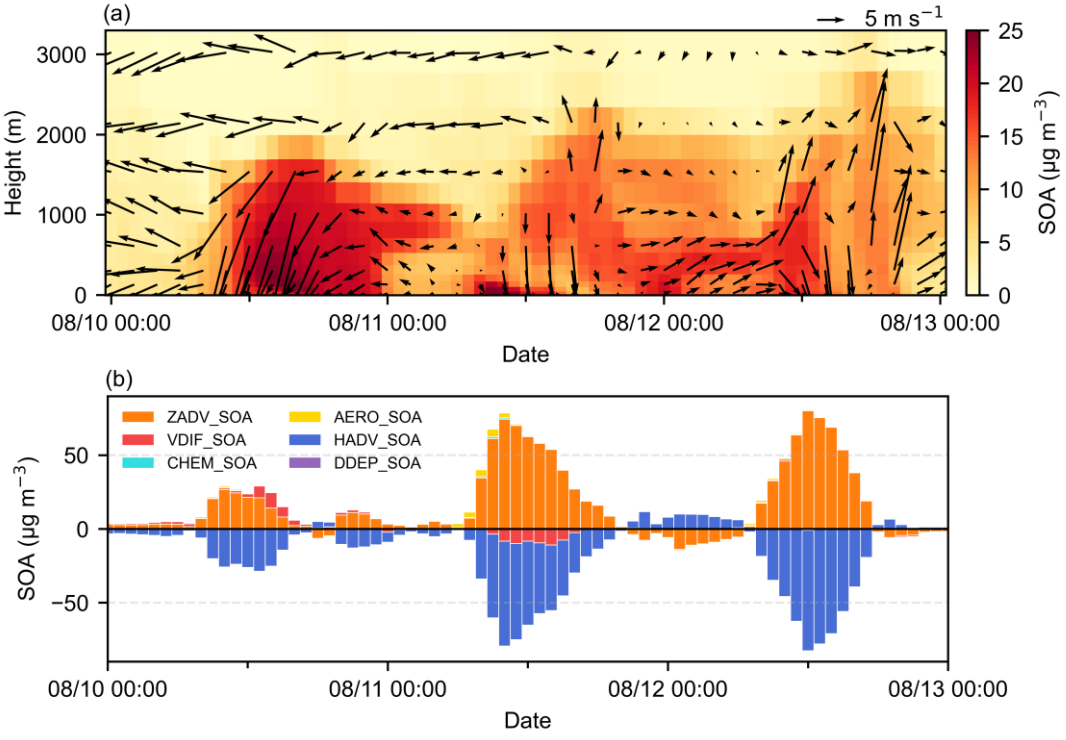


Figure 7. (a) Vertical time series of CMAQ-simulated SOA concentrations and WRF-simulated wind vectors (composed of the meridional component v and the vertical component w, with w magnified by a factor of 100 for visualization) at Taihu station during August 10–12. (b) CMAQ-simulated process analysis for SOA at Taihu station. The processes include vertical advection (ZADV), vertical diffusion (VDIF), chemical processes (CHEM), aerosol processes (AERO), horizontal advection (HADV), and dry deposition (DDEP).

4 Conclusion

This study investigated the formation and evolution of SOA over Taihu Lake during a summer field campaign in 2023, with particular focus on a pronounced SOA-driven pollution episode from August 10 to 12. OA was the dominant component of submicron aerosol, accounting for 56% of PM_1 on average and reaching 73.7 μg m^{-3}, or 78% of PM_1, during the episode. Source apportionment further showed that SOA contributed approximately 84% of total OA during the campaign and increased to 90% during the pollution episode, highlighting the dominant contribution of SOA during the episode.

The rapid SOA enhancement was associated with the combined influence of precursor availability, photochemical processing, and lake-induced meteorological conditions. The higher abundance of low-volatility and semi-volatile oxygenated organic molecules at Taihu Lake compared with the suburban SORPES station suggests an enhanced potential for gas-to-particle partitioning and SOA formation. The precursor analysis further indicates contributions from both anthropogenic emissions, particularly aromatic compounds transported from surrounding urban areas, and biogenic emissions from the lake–land interface. Elevated photochemical activity, indicated by higher O_x at Taihu Lake compared to surrounding land-surface sites,

https://doi.org/10.5194/egusphere-2026-6485
Preprint. Discussion started: 9 November 2026
© Author(s) 2026. CC BY 4.0 License.

promoted daytime SOA formation and oxidation, as evidenced by the rapid increase of both LO-OOA and MO-OOA. In addition to photochemical enhancement, lake-induced dynamics played a crucial role in facilitating this rapid surface accumulation. As supported by model simulations, the lake–land breeze circulation drove a consistent localized subsidence over the lake, which efficiently transported photochemically produced SOA from aloft toward the surface.

While the lack of direct biogenic VOC measurements from aquatic and shoreline vegetation precludes precise quantification of local precursor source strengths, the convergent observational and modeling evidence presented here shows that large inland lakes embedded within polluted urban–regional environments can provide favorable conditions for rapid SOA accumulation through coupled chemical and meteorological processes. These findings highlight the important yet underappreciated role of large inland water bodies in modulating regional aerosol formation and photochemical pollution, and emphasize the need to better represent lake–atmosphere interactions, mixed precursor chemistry, and boundary-layer dynamics in regional air quality predictions and pollution mitigation strategies.

Data availability

The O_x and $PM_{2.5}$ datasets are publicly available from https://air.cnemc.cn:18007. The GDAS meteorological data used to drive the HYSPLIT model are available at https://www.ready.noaa.gov/data/archives/gdas1/. The data supporting this study are available at https://doi.org/10.5281/zenodo.20340164. Other data related to this study are available upon request from Jiaping Wang (wangjp@nju.edu.cn)

Supplement link

The link to the supplement will be included by Copernicus, if applicable.

Author contributions

JPW, LY, and JDW designed this study. ZT analyzed data and drafted the manuscript. ZT, JPW, LY, CL, GY, JZ, NW, JBW, ZZ, BW, ChangZ, CaiZ, ZW, and JXW performed the field measurements. JPW, DD, and JDW supported the model simulations. QL assisted with the precursor classification of OOMs. JPW, JDW, DD, KD, YL, TL, WN, CY, LW and XH contributed to the data interpretation and review of the manuscript.

Competing interests

The authors declare that they have no conflict of interest

https://doi.org/10.5194/egusphere-2026-6485
Preprint. Discussion started: 9 November 2026
© Author(s) 2026. CC BY 4.0 License.

Disclaimer

Publisher's note: Copernicus Publications remains neutral with regard to jurisdictional claims made in the text, published maps, institutional affiliations, or any other geographical representation in this paper. While Copernicus Publications makes every effort to include appropriate place names, the final responsibility lies with the authors.

Acknowledgements

This work was supported through the National Natural Science Foundation of China (grant nos. 42475116 and 42422505). We acknowledge the support from Jiangsu Provincial Collaborative Innovation Center of Climate Change for their support of this work. We are grateful to the High-Performance Computing and Massive Data Center of Nanjing University for running the model on its blade cluster system.

Financial support

This work was supported by the National Natural Science Foundation of China (grant nos. 42475116 and 42422505).

References

Brook, J. R., Makar, P. A., Sills, D. M. L., Hayden, K. L., and McLaren, R.: Exploring the nature of air quality over southwestern Ontario: main findings from the Border Air Quality and Meteorology Study, Atmos. Chem. Phys., 13, 10461–10482, https://doi.org/10.5194/acp-13-10461-2013, 2013.

Carlton, A. G., Wiedinmyer, C., and Kroll, J. H.: A review of Secondary Organic Aerosol (SOA) formation from isoprene, Atmos. Chem. Phys., 9, 4987–5005, https://doi.org/https://doi.org/10.5194/acp-9-4987-2009, 2009.

Chen, Q., Miao, R., Geng, G., Shrivastava, M., Dao, X., Xu, B., Sun, J., Zhang, X., Liu, M., Tang, G., Tang, Q., Hu, H., Huang, R.-J., Wang, H., Zheng, Y., Qin, Y., Guo, S., Hu, M., and Zhu, T.: Widespread 2013-2020 decreases and reduction challenges of organic aerosol in China, Nat Commun, 15, 4465, https://doi.org/10.1038/s41467-024-48902-0, 2024.

Cleary, P. A., Dickens, A., McIlquham, M., Sanchez, M., Geib, K., Hedberg, C., Hupy, J., Watson, M. W., Fuoco, M., Olson, E. R., Pierce, R. B., Stanier, C., Long, R., Valin, L., Conley, S., and Smith, M.: Impacts of lake breeze meteorology on ozone gradient observations along Lake Michigan shorelines in Wisconsin, Atmospheric Environment, 269, 118834, https://doi.org/10.1016/j.atmosenv.2021.118834, 2022.

Ding, A., Nie, W., Huang, X., Chi, X., Sun, J., Kerminen, V.-M., Xu, Z., Guo, W., Petäjä, T., Yang, X., Kulmala, M., and Fu, C.: Long-term observation of air pollution-weather/climate interactions at the SORPES station: a review and outlook, Front. Environ. Sci. Eng., 10, 15, https://doi.org/10.1007/s11783-016-0877-3, 2016.

Ding, A., Huang, X., Nie, W., Chi, X., Xu, Z., Zheng, L., Xu, Z., Xie, Y., Qi, X., Shen, Y., Sun, P., Wang, J., Wang, L., Sun, J., Yang, X.-Q., Qin, W., Zhang, X., Cheng, W., Liu, W., Pan, L., and Fu, C.: Significant reduction of $PM_{2.5}$ in eastern China

https://doi.org/10.5194/egusphere-2026-6485
Preprint. Discussion started: 9 November 2026
© Author(s) 2026. CC BY 4.0 License.

due to regional-scale emission control: evidence from SORPES in 2011–2018, Atmospheric Chemistry and Physics, 19, 11791–11801, https://doi.org/10.5194/acp-19-11791-2019, 2019.

Donahue, N. M., Epstein, S. A., Pandis, S. N., and Robinson, A. L.: A two-dimensional volatility basis set: 1. organic-aerosol mixing thermodynamics, Atmos. Chem. Phys., 11, 3303–3318, https://doi.org/10.5194/acp-11-3303-2011, 2011.

Ehn, M., Thornton, J. A., Kleist, E., Sipilä, M., Junninen, H., Pullinen, I., Springer, M., Rubach, F., Tillmann, R., Lee, B., Lopez-Hilfiker, F., Andres, S., Acir, I.-H., Rissanen, M., Jokinen, T., Schobesberger, S., Kangasluoma, J., Kontkanen, J., Nieminen, T., Kurtén, T., Nielsen, L. B., Jørgensen, S., Kjaergaard, H. G., Canagaratna, M., Maso, M. D., Berndt, T., Petäjä, T., Wahner, A., Kerminen, V.-M., Kulmala, M., Worsnop, D. R., Wildt, J., and Mentel, T. F.: A large source of low-volatility secondary organic aerosol, Nature, 506, 476–479, https://doi.org/10.1038/nature13032, 2014.

Ervens, B., Turpin, B. J., and Weber, R. J.: Secondary organic aerosol formation in cloud droplets and aqueous particles (aqSOA): a review of laboratory, field and model studies, Atmos. Chem. Phys., 11, 11069–11102, https://doi.org/https://doi.org/10.5194/acp-11-11069-2011, 2011.

Feng, T., Zhao, S., Bei, N., Wu, J., Liu, S., Li, X., Liu, L., Qian, Y., Yang, Q., Wang, Y., Zhou, W., Cao, J., and Li, G.: Secondary organic aerosol enhanced by increasing atmospheric oxidizing capacity in Beijing–Tianjin–Hebei (BTH), China, Atmos. Chem. Phys., 19, 7429–7443, https://doi.org/10.5194/acp-19-7429-2019, 2019.

Gu, Y., Huang, R.-J., Duan, J., Xu, W., Lin, C., Zhong, H., Wang, Y., Ni, H., Liu, Q., Xu, R., Wang, L., and Li, Y. J.: Multiple pathways for the formation of secondary organic aerosol in the North China Plain in summer, Atmos. Chem. Phys., 23, 5419–5433, https://doi.org/10.5194/acp-23-5419-2023, 2023.

Hallquist, M., Wenger, J. C., Baltensperger, U., Rudich, Y., Simpson, D., Claeys, M., Dommen, J., Donahue, N. M., George, C., Goldstein, A. H., Hamilton, J. F., Herrmann, H., Hoffmann, T., Iinuma, Y., Jang, M., Jenkin, M. E., Jimenez, J. L., Kiendler-Scharr, A., Maenhaut, W., McFiggans, G., Mentel, T. F., Monod, A., Prevot, A. S. H., Seinfeld, J. H., Surratt, J. D., Szmigielski, R., and Wildt, J.: The formation, properties and impact of secondary organic aerosol: current and emerging issues, Atmos. Chem. Phys., 9, 5155–5236, https://doi.org/https://doi.org/10.5194/acp-9-5155-2009, 2009.

Hayden, K. L., Sills, D. M. L., Brook, J. R., O'Brien, J. M., Li, Q., and McLaren, R.: Aircraft study of the impact of lake-breeze circulations on trace gases and particles during BAQS-Met 2007, Atmos. Chem. Phys., 11, 10173–10192, https://doi.org/https://doi.org/10.5194/acp-11-10173-2011, 2011.

Herndon, S. C., Onasch, T. B., Wood, E. C., Kroll, J. H., Canagaratna, M. R., Jayne, J. T., Zavala, M. A., Knighton, W. B., Mazzoleni, C., Dubey, M. K., Ulbrich, I. M., Jimenez, J. L., Seila, R., De Gouw, J. A., De Foy, B., Fast, J., Molina, L. T., Kolb, C. E., and Worsnop, D. R.: Correlation of secondary organic aerosol with odd oxygen in Mexico City, Geophysical Research Letters, 35, 2008GL034058, https://doi.org/10.1029/2008GL034058, 2008.

Hu, W., Hu, M., Hu, W.-W., Zheng, J., Chen, C., Wu, Y., and Guo, S.: Seasonal variations in high time-resolved chemical compositions, sources, and evolution of atmospheric submicron aerosols in the megacity Beijing, Atmos. Chem. Phys., 17, 9979–10000, https://doi.org/10.5194/acp-17-9979-2017, 2017.

Huang, D. D., Kong, L., Gao, J., Lou, S., Qiao, L., Zhou, M., Ma, Y., Zhu, S., Wang, H., Chen, S., Zeng, L., and Huang, C.: Insights into the formation and properties of secondary organic aerosol at a background site in Yangtze River Delta region of China: Aqueous-phase processing vs. photochemical oxidation, Atmospheric Environment, 239, 117716, https://doi.org/10.1016/j.atmosenv.2020.117716, 2020.

Huang, R.-J., Zhang, Y., Bozzetti, C., Ho, K.-F., Cao, J.-J., Han, Y., Daellenbach, K. R., Slowik, J. G., Platt, S. M., Canonaco, F., Zotter, P., Wolf, R., Pieber, S. M., Bruns, E. A., Crippa, M., Ciarelli, G., Piazzalunga, A., Schwikowski, M., Abbaszade,

https://doi.org/10.5194/egusphere-2026-6485
Preprint. Discussion started: 9 November 2026
© Author(s) 2026. CC BY 4.0 License.

G., Schnelle-Kreis, J., Zimmermann, R., An, Z., Szidat, S., Baltensperger, U., Haddad, I. E., and Prévôt, A. S. H.: High secondary aerosol contribution to particulate pollution during haze events in China, Nature, 514, 218–222, https://doi.org/10.1038/nature13774, 2014.

Huang, R.-J., Li, Y. J., Chen, Q., Zhang, Y., Lin, C., Chan, C. K., Yu, J. Z., De Gouw, J., Tong, S., Jiang, J., Wang, W., Ding, X., Wang, X., Ge, M., Zhou, W., Worsnop, D., Boy, M., Bilde, M., Dusek, U., Carlton, A. G., Hoffmann, T., McNeill, V. F., and Glasius, M.: Secondary organic aerosol in urban China: A distinct chemical regime for air pollution studies, Science, 389, eadq2840, https://doi.org/10.1126/science.adq2840, 2025.

Jacobson, M. C., Hansson, H. -C., Noone, K. J., and Charlson, R. J.: Organic atmospheric aerosols: Review and state of the science, Reviews of Geophysics, 38, 267–294, https://doi.org/10.1029/1998RG000045, 2000.

Jimenez, J. L., Canagaratna, M. R., Donahue, N. M., Prevot, A. S. H., Zhang, Q., Kroll, J. H., DeCarlo, P. F., Allan, J. D., Coe, H., Ng, N. L., Aiken, A. C., Docherty, K. S., Ulbrich, I. M., Grieshop, A. P., Robinson, A. L., Duplissy, J., Smith, J. D., Wilson, K. R., Lanz, V. A., Hueglin, C., Sun, Y. L., Tian, J., Laaksonen, A., Raatikainen, T., Rautiainen, J., Vaattovaara, P., Ehn, M., Kulmala, M., Tomlinson, J. M., Collins, D. R., Cubison, M. J., E., Dunlea, J., Huffman, J. A., Onasch, T. B., Alfarra, M. R., Williams, P. I., Bower, K., Kondo, Y., Schneider, J., Drewnick, F., Borrmann, S., Weimer, S., Demerjian, K., Salcedo, D., Cottrell, L., Griffin, R., Takami, A., Miyoshi, T., Hatakeyama, S., Shimono, A., Sun, J. Y., Zhang, Y. M., Dzepina, K., Kimmel, J. R., Sueper, D., Jayne, J. T., Herndon, S. C., Trimborn, A. M., Williams, L. R., Wood, E. C., Middlebrook, A. M., Kolb, C. E., Baltensperger, U., and Worsnop, D. R.: Evolution of Organic Aerosols in the Atmosphere, Science, 326, 1525–1529, https://doi.org/10.1126/science.1180353, 2009.

Kuang, Y., He, Y., Xu, W., Yuan, B., Zhang, G., Ma, Z., Wu, C., Wang, C., Wang, S., Zhang, S., Tao, J., Ma, N., Su, H., Cheng, Y., Shao, M., and Sun, Y.: Photochemical Aqueous-Phase Reactions Induce Rapid Daytime Formation of Oxygenated Organic Aerosol on the North China Plain, Environ. Sci. Technol., 54, 3849–3860, https://doi.org/10.1021/acs.est.9b06836, 2020.

Lee, A. K. Y., Abbatt, J. P. D., Leaitch, W. R., Li, S.-M., Sjostedt, S. J., Wentzell, J. J. B., Liggio, J., and Macdonald, A. M.: Substantial secondary organic aerosol formation in a coniferous forest: observations of both day- and nighttime chemistry, Atmos. Chem. Phys., 16, 6721–6733, https://doi.org/10.5194/acp-16-6721-2016, 2016.

Levy, I., Makar, P. A., Sills, D., Zhang, J., Hayden, K. L., Mihele, C., Narayan, J., Moran, M. D., Sjostedt, S., and Brook, J.: Unraveling the complex local-scale flows influencing ozone patterns in the southern Great Lakes of North America, Atmos. Chem. Phys., 10, 10895–10915, https://doi.org/10.5194/acp-10-10895-2010, 2010.

Liu, T., Hong, Y., Li, M., Xu, L., Chen, J., Bian, Y., Yang, C., Dan, Y., Zhang, Y., Xue, L., Zhao, M., Huang, Z., and Wang, H.: Atmospheric oxidation capacity and ozone pollution mechanism in a coastal city of southeastern China: analysis of a typical photochemical episode by an observation-based model, Atmos. Chem. Phys., 22, 2173–2190, https://doi.org/10.5194/acp-22-2173-2022, 2022.

Liu, Y., Nie, W., Li, Y., Ge, D., Liu, C., Xu, Z., Chen, L., Wang, T., Wang, L., Sun, P., Qi, X., Wang, J., Xu, Z., Yuan, J., Yan, C., Zhang, Y., Huang, D., Wang, Z., Donahue, N. M., Worsnop, D., Chi, X., Ehn, M., and Ding, A.: Formation of condensable organic vapors from anthropogenic and biogenic volatile organic compounds (VOCs) is strongly perturbed by NO_x in eastern China, Atmos. Chem. Phys., 21, 14789–14814, https://doi.org/10.5194/acp-21-14789-2021, 2021.

Liu, Y., Liu, C., Nie, W., Li, Y., Ge, D., Chen, L., Zhu, C., Wang, L., Zhang, Y., Liu, T., Qi, X., Wang, J., Huang, D., Wang, Z., Yan, C., Chi, X., and Ding, A.: Exploring condensable organic vapors and their co-occurrence with $PM_{2.5}$ and O_3 in winter in Eastern China, Environ. Sci.: Atmos., 3, 282–297, https://doi.org/10.1039/D2EA00143H, 2023.

https://doi.org/10.5194/egusphere-2026-6485
Preprint. Discussion started: 9 November 2026
© Author(s) 2026. CC BY 4.0 License.

Lu, X., Hong, J., Zhang, L., Cooper, O. R., Schultz, M. G., Xu, X., Wang, T., Gao, M., Zhao, Y., and Zhang, Y.: Severe Surface Ozone Pollution in China: A Global Perspective, Environ. Sci. Technol. Lett., 5, 487–494, https://doi.org/10.1021/acs.estlett.8b00366, 2018.

Ming, L., Jin, L., Li, J., Fu, P., Yang, W., Liu, D., Zhang, G., Wang, Z., and Li, X.: $PM_{2.5}$ in the Yangtze River Delta, China: Chemical compositions, seasonal variations, and regional pollution events, Environmental Pollution, 223, 200–212, https://doi.org/10.1016/j.envpol.2017.01.013, 2017.

Mohr, C., Thornton, J. A., Heitto, A., Lopez-Hilfiker, F. D., Lutz, A., Riipinen, I., Hong, J., Donahue, N. M., Hallquist, M., Petäjä, T., Kulmala, M., and Yli-Juuti, T.: Molecular identification of organic vapors driving atmospheric nanoparticle growth, Nat Commun, 10, 4442, https://doi.org/10.1038/s41467-019-12473-2, 2019.

Nie, W., Yan, C., Huang, D. D., Wang, Z., Liu, Y., Qiao, X., Guo, Y., Tian, L., Zheng, P., Xu, Z., Li, Y., Xu, Z., Qi, X., Sun, P., Wang, J., Zheng, F., Li, X., Yin, R., Dallenbach, K. R., Bianchi, F., Petäjä, T., Zhang, Y., Wang, M., Schervish, M., Wang, S., Qiao, L., Wang, Q., Zhou, M., Wang, H., Yu, C., Yao, D., Guo, H., Ye, P., Lee, S., Li, Y. J., Liu, Y., Chi, X., Kerminen, V.-M., Ehn, M., Donahue, N. M., Wang, T., Huang, C., Kulmala, M., Worsnop, D., Jiang, J., and Ding, A.: Secondary organic aerosol formed by condensing anthropogenic vapours over China's megacities, Nat. Geosci., 15, 255–261, https://doi.org/10.1038/s41561-022-00922-5, 2022.

Onasch, T. B., Trimborn, A., Fortner, E. C., Jayne, J. T., Kok, G. L., Williams, L. R., Davidovits, P., and Worsnop, D. R.: Soot Particle Aerosol Mass Spectrometer: Development, Validation, and Initial Application, Aerosol Science and Technology, 46, 804–817, https://doi.org/10.1080/02786826.2012.663948, 2012.

Paatero, P. and Tapper, U.: Positive matrix factorization: A non-negative factor model with optimal utilization of error estimates of data values, Environmetrics, 5, 111–126, https://doi.org/10.1002/env.3170050203, 1994.

RenHe, Z., Li, Q., and Zhang, R.: Meteorological conditions for the persistent severe fog and haze event over eastern China in January 2013, Sci. China Earth Sci., 57, 26–35, https://doi.org/10.1007/s11430-013-4774-3, 2014.

Shao, M., Wei, Y., Lv, S., Liao, Z., Zou, J., and Zhu, J.: Contribution and Mechanisms of BVOCs Emitted From a Typical Large Lake With Algal Bloom to O_3 Levels in Lakeside Urban Areas, JGR Atmospheres, 130, e2024JD042248, https://doi.org/10.1029/2024JD042248, 2025.

Stein, A. F., Draxler, R. R., Rolph, G. D., Stunder, B. J. B., Cohen, M. D., and Ngan, F.: NOAA's HYSPLIT Atmospheric Transport and Dispersion Modeling System, Bulletin of the American Meteorological Society, 96, 2059–2077, https://doi.org/10.1175/BAMS-D-14-00110.1, 2015.

Sun, Y., Luo, H., Li, Y., Zhou, W., Xu, W., Fu, P., and Zhao, D.: Atmospheric organic aerosols: online molecular characterization and environmental impacts, npj Clim Atmos Sci, 8, 305, https://doi.org/10.1038/s41612-025-01199-2, 2025.

Tröstl, J., Chuang, W. K., Gordon, H., Heinritzi, M., Yan, C., Molteni, U., Ahlm, L., Frege, C., Bianchi, F., Wagner, R., Simon, M., Lehtipalo, K., Williamson, C., Craven, J. S., Duplissy, J., Adamov, A., Almeida, J., Bernhammer, A.-K., Breitenlechner, M., Brilke, S., Dias, A., Ehrhart, S., Flagan, R. C., Franchin, A., Fuchs, C., Guida, R., Gysel, M., Hansel, A., Hoyle, C. R., Jokinen, T., Junninen, H., Kangasluoma, J., Keskinen, H., Kim, J., Krapf, M., Kürten, A., Laaksonen, A., Lawler, M., Leiminger, M., Mathot, S., Möhler, O., Nieminen, T., Onnela, A., Petäjä, T., Piel, F. M., Miettinen, P., Rissanen, M. P., Rondo, L., Sarnela, N., Schobesberger, S., Sengupta, K., Sipilä, M., Smith, J. N., Steiner, G., Tomè, A., Virtanen, A., Wagner, A. C., Weingartner, E., Wimmer, D., Winkler, P. M., Ye, P., Carslaw, K. S., Curtius, J., Dommen, J., Kirkby, J., Kulmala, M., Riipinen, I., Worsnop, D. R., Donahue, N. M., and Baltensperger, U.: The role of low-volatility organic compounds in initial particle growth in the atmosphere, Nature, 533, 527–531, https://doi.org/10.1038/nature18271, 2016.

https://doi.org/10.5194/egusphere-2026-6485
Preprint. Discussion started: 9 November 2026
© Author(s) 2026. CC BY 4.0 License.



Ulbrich, I. M., Canagaratna, M. R., Zhang, Q., Worsnop, D. R., and Jimenez, J. L.: Interpretation of organic components from Positive Matrix Factorization of aerosol mass spectrometric data, Atmos. Chem. Phys., 9, 2891–2918, https://doi.org/https://doi.org/10.5194/acp-9-2891-2009, 2009.

Wang, Y., Clusius, P., Yan, C., Dällenbach, K., Yin, R., Wang, M., He, X.-C., Chu, B., Lu, Y., Dada, L., Kangasluoma, J., Rantala, P., Deng, C., Lin, Z., Wang, W., Yao, L., Fan, X., Du, W., Cai, J., Heikkinen, L., Tham, Y. J., Zha, Q., Ling, Z., Junninen, H., Petäjä, T., Ge, M., Wang, Y., He, H., Worsnop, D. R., Kerminen, V.-M., Bianchi, F., Wang, L., Jiang, J., Liu, Y., Boy, M., Ehn, M., Donahue, N. M., and Kulmala, M.: Molecular Composition of Oxygenated Organic Molecules and Their Contributions to Organic Aerosol in Beijing, Environ. Sci. Technol., 56, 770–778, https://doi.org/10.1021/acs.est.1c05191, 2022.

Xie, M., Zhan, C., Zhan, Y., Shi, J., Luo, Y., Zhang, M., Liu, Q., and Shen, F.: Spatiotemporal Variability of Air Stagnation and its Relation to Summertime Ozone in the Yangtze River Delta of China, Front. Environ. Sci., 9, 783524, https://doi.org/10.3389/fenvs.2021.783524, 2021.

Ying, Q., Li, J., and Kota, S. H.: Significant Contributions of Isoprene to Summertime Secondary Organic Aerosol in Eastern United States, Environ. Sci. Technol., 49, 7834–7842, https://doi.org/10.1021/acs.est.5b02514, 2015.

Yu, Y., Li, C., Shen, W., Wang, Z., Xu, P., and Yu, H.: Volatile compounds released by microalgae-water phase from Taihu Lake in China, Harmful Algae, 84, 56–63, https://doi.org/10.1016/j.hal.2019.01.009, 2019.

Zhang, J., Wang, J., Sun, Y., Li, J., Ninneman, M., Ye, J., Li, K., Crandall, B., Mao, J., Xu, W., Schwab, M. J., Li, W., Ge, X., Chen, M., Ying, Q., Zhang, Q., and Schwab, J. J.: Insights from ozone and particulate matter pollution control in New York City applied to Beijing, npj Clim Atmos Sci, 5, 85, https://doi.org/10.1038/s41612-022-00309-8, 2022.

Zhang, L., Zhu, B., Gao, J., and Kang, H.: Impact of Taihu Lake on city ozone in the Yangtze River Delta, Adv. Atmos. Sci., 34, 226–234, https://doi.org/10.1007/s00376-016-6099-6, 2017.

Zhou, X., Li, M., Huang, X., Liu, T., Zhang, H., Qi, X., Wang, Z., Qin, Y., Geng, G., Wang, J., Chi, X., and Ding, A.: Urban meteorology–chemistry coupling in compound heat–ozone extremes, Nat Cities, https://doi.org/10.1038/s44284-025-00302-1, 2025.